JOURNAL OF PROPULSION AND POWER
Vol. 12, No. 3, May–June 1996

Semiempirical Correlations of NO_x Emissions from Utility Combustion Turbines with Inert Injection

D. M. Newburry* and A. M. Mellor†
Vanderbilt University, Nashville, Tennessee 37235-1592

Semiempirical models describe the dominant subprocesses involved in pollutant emissions by assigning specific times to the fuel evaporation, chemistry, and turbulent mixing. Linear ratios of these times with model constants established by correlating data from combustors with different geometries, inlet conditions, fuels, and fuel injectors can then be employed to make a priori predictions. In this work, NO_x emissions from two heavy-duty, dual-fuel (natural gas and fuel oil no. 2) diffusion-flame combustors designated A and B are examined. The data are first predicted and then correlated using the existing semiempirical characteristic time model. Heterogeneous effects are found to be significant, in contrast to previous results with aircraft engine combustors. Inert injection for NO_x control is modeled as thermal, and two limiting cases are proposed that bound the measured data. An empirically selected effective inert injection flame temperature was substituted for the stoichiometric flame temperature used to estimate the thermal NO formation rate in the model. This procedure correlated all of the measured NO_xEI with a standard deviation of 1.02 g NO_2/kg fuel that results from a curvature in the emissions index vs load data for combustor B. Removing the curvature empirically improves the combined correlation to a standard deviation of 0.28 g/kg (approximately 3.2 parts per million volume dry at 15% O_2).

Nomenclature

a = molar ratio of water-to-fuel flow rate
d_{comb} = maximum combustor diameter, cm
d_0 = initial drop diameter, Sauter mean diameter, m
E_{no} = activation energy for thermal NO formation, 135 kcal/gmol
k_{no} = empirical coefficient for droplet evaporation term in NO_x models
l_{no} = characteristic length for NO_x emissions, cm
l_{sec} = secondary length, distance downstream from fuel injector tip to centerline of secondary air addition holes
M = molecular weight, g/gmol
$\dot{m}_a$ = total combustor airflow rate, kg/s
$\dot{m}_{apz}$ = primary zone airflow rate, kg/s
$\dot{m}_{fuel}$ = combustor fuel flow rate, kg/h
$\dot{m}_{H_2O}$ = combustor water/steam flow rate, kg/h
NO_x = oxides of nitrogen, NO and NO_2
NO_xEI = oxides of nitrogen emissions index, g NO_x as NO_2/kg fuel
P = pressure, atm
R = universal gas constant, 8.206×10^{-5} atm·m³/gmol·K or 1.986 cal/gmol·K
r = correlation coefficient
T = temperature, K
$T_{\phi=1}$ = adiabatic flame temperature at the overall equivalence ratio, K
T_ϕ = adiabatic stoichiometric flame temperature, K
u_r = relative velocity, assumed constant, between fuel drop and air, m/s
V_{ref} = reference velocity, velocity of combustor inlet airflow at maximum combustor cross-sectional area, m/s
V_ϕ = flame zone velocity at the given equivalence ratio, m/s
$V_{\phi=1}$ = stoichiometric flame zone velocity, m/s
β_{conv} = fuel droplet evaporation coefficient corrected for forced convection, m²/s
θ = swirl angle
σ_y = standard deviation of the y values for the observed values of x
τ_{eb} = evaporation time, ms
τ_{no} = characteristic kinetic time for thermal NO formation, ms
$\tau_{sl,no}$ = residence time in the final, near stoichiometric shear layer, ms
ϕ = fuel–air equivalence ratio

Subscripts
a = air
all = all inert going to the stoichiometric eddies
dry = no inert injection
fuel = fuel
H_2O = water or steam
in = inlet value
no = nitric oxide
pred = predicted
pz = primary zone
s = value at liquid saturation point
unif = inert distributed uniformly throughout combustion
1st row = at the first row of air addition holes
∞ = ambient value

Received April 11, 1995; revision received Oct. 3, 1995; accepted for publication Nov. 6, 1995.

*Graduate Research Assistant, Mechanical Engineering; currently Engineer, Combustion Turbine Engineering, Westinghouse Electric Corporation, Orlando, FL.

†Centennial Professor, Mechanical Engineering. Associate Fellow AIAA.

Introduction

STRICTER emissions standards enacted for almost all combustion devices including gas turbines have led industries to modify their designs to reduce the emissions of nitrogen oxides, carbon monoxide, and unburned hydrocarbons. Developing accurate analytical models to predict these emissions in terms of gas-turbine combustor geometry, fuel and the fuel injection method, and combustor inlet conditions can reduce the time and cost of the developmental process. Also, such

models may be used as a substitute for emissions measurement instrumentation or as a way to verify actual emissions and performance when a monitoring system is available.[1]

Computational fluid dynamics (CFD) codes are becoming widely used in industry to estimate combustor flow and temperature patterns and species concentrations within either existing combustors or future designs as a means of eliminating some of the time and expense of new combustor development. However, because of the very complex nature of the processes these models attempt to simulate, submodels with empirical model constants must be introduced to account for turbulence, kinetics, fuel evaporation, etc. If CFD codes are used in conjunction with testing to ensure the results are reasonable, they can nevertheless expedite the combustor development process through eliminating unnecessary testing by showing which designs have the best possibility of giving the desired results.

Semiempirical models fall between detailed computational and purely empirical methods. They attempt to simplify the complex combustion processes that occur in gas-turbine combustors into the relevant subprocesses in the important region of the flow, important to the particular operating parameter of interest. For pollutant emissions modeling, specific times are assigned to fuel evaporation, chemistry, and turbulent mixing, all evaluated in the shear layer adjacent to the recirculating region in the combustor primary zone. Linear combinations and/or ratios of these times are used to correlate measured pollutant emissions from combustors with different geometries, inlet conditions, fuels, and fuel injectors to establish model constants. These constants may then be used for predictions for other geometries, fuels, etc. The constants can be fine-tuned when data become available for a new combustor, or when an improved correlation is desired for a particular combustor. However, caution must be exercised when extrapolating these equations to designs radically different than those for which they were developed, as with any empirically based approach. Derr and Mellor[2] provide a recent summary of the state of semiempirical modeling, including the characteristic time model (CTM).

In this work, the CTM (Ref. 3) was used to predict dry (i.e., no inert injection) thermal NO_x emissions data from two diffusion-flame combustors, designated A and B, used in turbines designed for power generation in the 100–150-MW range, and produced by two U.S. manufacturers. Because these heavy-duty, large-scale combustors exhibit effects of finite rate fuel evaporation on NO_x emissions when oil-fired, it was necessary to modify the CTM prediction equation developed for smaller combustors.[4] The results were also compared[4] to those from models developed by Lefebvre[5] and Rizk and Mongia[6]; the modified CTM gave the best correlation of the dry data. None of the models has been utilized previously to correlate data where inert injection is used to suppress NO_x emissions. Therefore, based on the dry data results, the CTM was the model selected to correlate the inert injection data.

Characteristic Time Model

The CTM was first developed for spray flames on laboratory flameholders[3,7] and was then extended to gas turbine diffusion-flame combustors for emissions of thermal nitric oxide, carbon monoxide, and unburned hydrocarbons.[8,9] The model has been validated to provide a single thermal NO_x emissions correlation for automotive, helicopter, industrial, and aircraft gas-turbine applications.[10,11]

The thermal NO_x CTM focuses on the final, near-stoichiometric shear layer, which has been previously defined[12] as the predominate area for postflame NO formation in conventional diffusion-flame combustors. This shear layer surrounds the recirculation zone in the front portion of the combustor.[2] The kinetic time for NO formation τ_{no} is expressed in inverse Arrhenius form and is the characteristic time required for thermal nitric oxide to form

$$\tau_{no} = 10^{-12} \exp(E_{no}/RT_{\phi=1}), \text{ ms} \quad (1)$$

where the pre-exponential factor, 10^{-12} ms, was chosen so that τ_{no} is on the order of milliseconds and the activation energy E_{no} was found empirically to be 135,000 cal/gmol for laboratory flameholders,[13] based on a similar correlation[14] of data from a large number of diffusion-flame combustors. This value is very close to the calculated activation energy for the Zeldovich mechanism,[15] assuming N is in steady state and O and O_2 are in equilibrium (135,500 cal/gmol[10]), and has been used previously in CTM correlations for widely differing gas-turbine combustors.[2]

The characteristic lifetime of an eddy in the NO-forming region of a combustor is defined

$$\tau_{sl,no} = l_{no}/V_{\phi=1} \times 1000, \text{ ms} \quad (2)$$

where the assumption is made that the formation of thermal NO occurs primarily at the trailing edge of the shear layer. The introduction of secondary air terminates the recirculation zone and quenches thermal NO formation because of the penetration jets closing the shear layer to the centerline. Therefore, l_{no} is defined:

$$l_{no}^{-1} = (l_{sec}/\cos\theta)^{-1} + (d_{comb})^{-1}, \text{ 1/m} \quad (3)$$

The combustor diameter is included to account for the radial extent of the shear layer based on a study of similar combustors with different diameters.[8] Swirl (vane angle θ) increases NO emissions[11] since the residence time in the shear layer is increased.

The velocity $V_{\phi=1}$ is used to estimate the velocity of stoichiometric eddies traveling down the shear layer and can be expressed as a fraction of the reference velocity, based on maximum combustor cross-sectional area:

$$V_{ref} = \frac{\dot{m}_a R T_{in}}{P_{in} M_a (\pi/4) d_{comb}^2}, \text{ m/s} \quad (4)$$

$$V_{\phi=1} = (\dot{m}_{apz}/\dot{m}_a)(T_{\phi=1}/T_{in})V_{ref}, \text{ m/s} \quad (5)$$

For thermal NO emissions, the airflow to the primary zone is defined as entering from five locations: 1) dome air, 2) swirler air, 3) primary jet air, 4) film air deflected into the primary zone, and 5) a fraction of the secondary jet air that recirculates into the primary zone.[10]

Finite rate fuel evaporation decreases NO formation from that expected for completely vaporized liquid fuel,[7] and is modeled by adding a fuel droplet lifetime τ_{eb} (multiplied by an empirical constant k_{no}) to the kinetic time for NO formation. Evaporation times were calculated using the d^2 law of Godsave[16]:

$$\tau_{eb} = d_0^2/\beta_{conv} \quad (6)$$

where d_0 is taken as the spray Sauter mean diameter (SMD) and β_{conv} is the evaporation coefficient corrected for forced convection effects with an empirical correlation from Frössling.[17] To be consistent with previous CTM correlations, the assumptions used by Leonard and Mellor[18] for calculating evaporation coefficients [i.e., T_∞ = 1000 K, u_r = 50 m/s, and T_s = mean (50% recovered) boiling point] were also made here.

The CTM predicting equation for NO is given[7] as a Damköhler number modified for heterogeneous effects:

$$NO_xEI = 4.5\tau_{sl,no}/(\tau_{no} + k_{no}\tau_{eb}) \quad (7)$$

The empirical constant k_{no} in the CTM was recommended to be 0.1 by Tuttle et al.,[7] based on data from a laboratory combustor. This value was not found appropriate for gas-turbine combustors, as the value of 0.05 gave the best correlation of the data in this study.[4] Also, the slope of 4.5 was determined

by Mellor and Washam,[11] who assumed negligible evaporation effects ($k_{no} = 0$) for the combustors studied previously. This CTM predicting Eq. (7) for thermal NO_x with $k_{no} = 0$ has an estimated[2] standard deviation of ± 3 g/kg. Other than the explicit pressure dependence given by Eq. (4), a nonlinear variation with combustor pressure is implied by Eq. (7), because of the appearance of $T_{\phi=1}$ in both Eqs. (1) and (5).

Inert Injection Effects

Kinetic pathways for the formation of NO include the Zeldovich (or thermal) mechanism,[15] the prompt mechanism,[19] and the nitrous-oxide mechanism.[20] In conventional diffusion-flame combustors, the NO is largely produced via the Zeldovich (or thermal) mechanism as a result of chemical combination of O_2 and N_2 in the air because of high flame temperatures.[15] Thus, the majority of the NO is formed in the eddies at the trailing edge of the shear layer, where near-stoichiometric mixtures are burning, and the appropriate temperature for modeling NO formation in a conventional diffusion flame combustor is the stoichiometric $T_{\phi=1}$ of the fuel in use[3] [see Eqs. (1) and (5)].

Inert injection reduces NO primarily through a reduction in these peak flame temperatures. Gross combustor parameters such as swirl, overall equivalence ratio, inlet temperature, etc., weakly influence NO_x abatement effectiveness consistent with stoichiometric diffusion flame combustion.[21] The inert absorbs heat from the reacting species and dilutes the fuel/air mixture. This causes a large decrease in the amount of NO produced via the thermal mechanism. Thermal NO is much more sensitive to steam/water injection than prompt NO that varies with the stoichiometric equilibrium concentration[19] of NO and does not display much reduction with water injection.[22] There are rapidly diminishing returns on NO reduction when injecting more than 1 kg of water per kg of hydrocarbon fuel,[21,22] and Toof[22] concluded most of the remaining NO is prompt. Bahr and Lyon[23] recommend a value of 0.8 as the upper limit for the water-to-fuel ratio, as the NO_x reductions achieved above this value are no longer worth the economic penalty.

To accurately model the effects of water injection, Toof[22] suggested a prompt NO calculation must be included. He found that a thermal NO calculation based on the Zeldovich mechanism and equilibrium hydrocarbon chemistry predicted about a 95% reduction rather than the 80% reduction he observed for a distillate fuel with no fuel-bound nitrogen. A similar result was found by Touchton[21] for methane fuel. Neither investigator considered either the N_2O mechanism or N_2O emissions.

Toof[22] also noted that normalized NO_x reductions reported for a given fuel are not universal, as more thermal NO is formed at higher pressures and temperatures. As a result, a greater percentage reduction in NO_x is obtained at higher combustor inlet pressure and temperature, even though the relative amount of fuel and water is the same. Thus, percentage reductions in NO_x with steam/water injection are functions of the operating conditions as well as the fuel composition, and so the percentage is not a specific curve for a given fuel, but rather a family of curves varying with operating conditions. Touchton[21] also found this to be the case, for he obtained slightly greater effectiveness in an aeroderivative as opposed to a heavy-duty utility gas turbine because of the higher combustor inlet temperatures and pressures in the former.

Touchton[21] originally attributed differences between his kinetic predictions and experimental results to a lack of proper fuel and steam mixing, but later observed no significant improvement in NO_x abatement when the steam and fuel were premixed. In addition, head-end steam injection vs steam injection through the primary holes vs mixed steam and fuel injection, produced similar reductions; steam entering with either air or fuel was also equally effective in decreasing NO_x. However, no reduction was observed with inert injection through downstream rows of holes.

The CTM has not been used previously to model the effects of inert injection. However, interpreting Touchton's mixing results in terms of the shear-layer trailing edge, that is, the zone of maximum thermal NO formation, water/steam injection locations that are equally effective at reducing NO formation are distributing the inert in the same way to the downstream regions of the shear layer. Since fuel and primary air both participate in the shear layer, it follows that steam injection with either will impact on the thermal NO formation kinetics, but inert injection too far downstream will not. In fact, the maximum possible reduction requires inserting all inert into the stoichiometric, NO-forming eddies only. This is impossible from a practical sense in that no matter where the water is injected into the combustor, part of it will always mix with nonstoichiometric zones of the shear layer. The opposite extreme is the case where steam is injected into the compressor discharge air, and only a portion of the steam reaches the NO formation zone, while the remainder flows through cooling slots and the liner dilution holes. This is identical to what occurs with ambient humidity, and forms the basis for a second conceptual bound on NO_x emissions. Many investigators have examined ambient humidity effects on NO_x production from a theoretical and empirical standpoint.[24-27] In the following section, these two thermodynamic limits on NO_x reductions with inert injection are developed quantitatively and compared with measured data for combustion turbines.

Limiting Cases for NO_x Reductions via Inert Injection

As noted, it is postulated that the maximum reduction is achieved if all of the inert could be placed in the stoichiometric eddies of the shear layer where the majority of the thermal NO is formed. In contrast, the minimum NO_x reduction will be achieved when the diluent is mixed completely throughout all of the combustor air.

These two limiting cases may be estimated by adding the appropriate amounts of inert into the calculation of $T_{\phi=1}$, which is used to estimate the thermal NO formation rate in the CTM. Following Touchton,[28] effects of water/steam injection on species concentrations, including that of hydroxyl, are neglected. All temperature calculations were made using the thermochemical code STANJAN[29] with reactant proportions for all inert to the stoichiometric eddies $T_{\phi=1,all}$, and for uniform water distribution $T_{\phi=1,unif}$ for methane fuel specified as follows.

The stoichiometric reaction for methane provides $T_{\phi=1}$:

$$CH_4 + 9.52(0.21O_2 + 0.79N_2) \rightarrow \cdots \quad (8)$$

For $T_{\phi=1,all}$, all of the inert is assumed intimately mixed with the stoichiometric, NO-forming eddies. The ratio of water-to-fuel in the combustor on a molar basis a is given by

$$a = (\dot{m}_{H_2O}/\dot{m}_{fuel})(M_{fuel}/M_{H_2O}) \quad (9)$$

Thus, $T_{\phi=1,all}$ is calculated with the reaction

$$CH_4 + (a)H_2O + 9.52(0.21O_2 + 0.79N_2) \rightarrow \cdots \quad (10)$$

where the appropriate fuel, air, and water/steam inlet temperatures are used, as well as the proper phase of the inert injectant to include the latent heat of vaporization for water injection.

For $T_{\phi=1,unif}$, the injected water is mixed uniformly throughout all of the combustor air. Therefore, only the fraction ϕ, the fuel/air equivalence ratio, of that in Eq. (9) is available to dilute the stoichiometric eddies. In this case the appropriate stoichiometric flame temperature is computed from

$$CH_4 + (a\phi)H_2O + 9.52(0.21O_2 + 0.79N_2) \rightarrow \cdots \quad (11)$$

where, again, the appropriate fuel, air, and water/steam inlet temperatures, as well as the proper injectant phase must be used. It is clear that the reactants in Eq. (10) will result in lower stoichiometric temperatures with inert injection than will those in Eq. (11), since $\phi < 1$.

The fractional NO_x emissions for natural gas fuel predicted for both of these cases based on the characteristic time model are shown in Fig. 1 for a hypothetical combustor burning pure CH_4 at a constant load over a range of injected water-to-fuel mass flow ratios. The overall fuel–air equivalence ratio for the case in Fig. 1 with no water injection is 0.2, which is increased as required with increased water-to-fuel ratios to keep the firing temperature constant. The solid lines are the two cases discussed previously. The best-case inert-to-stoichiometric-eddies model predicts zero thermal NO_x emissions at a water-to-fuel flow rate ratio of 2.5, while the presumably worst-case uniform-water-injection model suggests an 80% reduction in thermal NO_x under the same conditions. However, as discussed previously, the amount of total NO_x reduction achievable through water/steam injection may be limited by NO formation mechanisms other than thermal.[22]

As an example of this limiting case, we have used the lean premixed (LP) characteristic time model of Newburry and Mellor[30] that represents a correlation of LP NO_x measurements obtained in the 10- to 30-atm regime with a perforated plate flameholder and C_3H_8 as fuel. As such, this CTM may reflect contributions from both prompt NO and NO formed via the N_2O mechanism.[30] The temperature used in this model is the burner outlet value at the overall equivalence ratio T_ϕ, and so substitution of the various parameters in the LP NO_x model will yield the dashed horizontal line in Fig. 1, because burner outlet temperature and firing temperature are held constant as water-to-fuel flow ratio is increased. We omit the detailed equations because only the relative placement of the dashed LP NO_x and the best- and worst-case NO_x predictions in the figure are of interest here to illustrate the conclusions of both Touchton[21] and Toof.[22]

There is also a maximum amount of water/steam that may be injected, since too much will eventually blow out the flame. Using the blowoff model of Derr and Mellor[31] with $T_{\phi=1,all}$ to approximate the worst case, it was found that blowoff in the example situation was not predicted until water-to-fuel ratios of greater than seven were used. Since steam has less heat capacity, blowoff is not expected in practice with either phase of the inert. Note, however, that pressure oscillations are usually encountered prior to the blowout limit.[21,32]

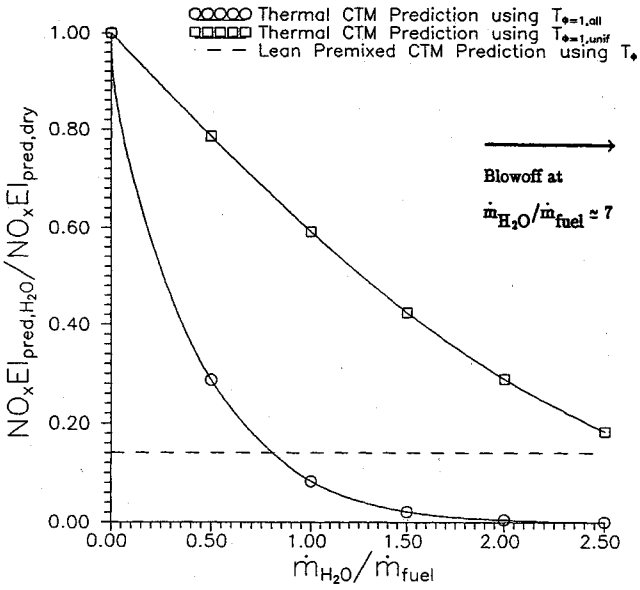

Fig. 1 Limiting cases for water injection in a hypothetical combustor at a constant power level burning pure methane with an overall equivalence ratio of 0.2 for the case without water injection. Since the fractional reduction is presented, only parameters affecting the flame temperatures and kinetic times influence the magnitudes graphed. These additional parameters were taken as T_{in} = 600 K and P_{in} = 10 atm.

Combustor Information

Combustors A and B are of the can- or tubo-annular type, and the fuel is delivered by a dual-fuel (natural gas or fuel oil) injection system that is also capable of supplying water or steam for NO_x emissions control. These nonaeroderivative combustors are similar to aircraft combustors in some aspects, but operate with a nearly constant airflow rate for all power settings, while aircraft combustors generally utilize a constant reference velocity. Also, stationary cycles are usually limited to lower compressor pressure ratios to increase hot section durability.

The NO_x emissions data, geometries, fuel injector characteristics, and operating conditions for combustors A and B were provided by their respective manufacturers [although much of this information is proprietary, the reader may consult Refs. 8 and 9 to examine typical datum bases for other burners used to develop Eq. (7) with $k_{no} = 0$]. Both natural gas and fuel oil data, with and without water and steam injection, were given, with the exception of steam injection data for combustor A. For combustor B, data were available over a range of inert-to-fuel mass flow ratios from zero to approximately one, whereas for combustor A, the data were characterized by either near unity or zero water-to-fuel ratios. All additional data required for the CTM analysis,[10] such as combustor dimensions, inlet conditions, and injector and fuel specifications, were furnished as well. Although requested, no statistical information on the accuracy of the emissions data was reported by either manufacturer.

Fuel files were constructed for each of the specified fuels for the thermochemical code, STANJAN,[29] which was used to calculate all of the equilibrium adiabatic flame temperatures required by the model. Since the reported emissions data for combustor B were field-test averages, one specific fuel composition could not be reported for either natural gas or fuel oil. Thus, average fuel compositions were provided.

Sauter mean diameters for the combustor A fuel injector operating with no. 2 fuel oil at firing conditions were provided by the manufacturer. However, for combustor B, no information on the Sauter mean diameters with oil firing was available. Therefore, the SMDs were estimated with an empirical correlation from Elkotb et al.,[33] which was updated in Lefebvre.[34] Since the correlation used to calculate the SMDs was not developed for the specific injector geometry of combustor B, the corresponding evaporation times may be less accurate.

NO_x Emissions Predictions and Correlations

Figure 2 is the CTM performance comparison with k_{no} chosen equal to 0.05 to maximize the correlation coefficient for the combined combustor data. Combustor A data are represented with solid symbols, whereas those for combustor B are shown with open symbols. Circles represent gas firing and squares oil firing. In general, for both combustors, NO_x emissions increase with increasing load (i.e., move further from the origin), and, at a given load, are higher for oil-firing than gas-firing. The result that k_{no} in Eq. (7) is positive indicates that oil-fired NO_x emissions are higher than those shown in Fig. 2 for both combustors when based on the fuel-oil stoichiometric flame temperature and $k_{no} = 0$. Consequently, less volatile and more viscous fuels, in conjunction with moderate atomization, tend to reduce NO_x (and increase combustion inefficiency) from values computed assuming the spray vaporizes completely prior to quenching the combustion and NO formation.[7]

The solid best-fit line in Fig. 2 with $k_{no} = 0.05$ is given in the figure, as is the estimated standard deviation of the original prediction equation (±3 g/kg), with dashed lines. All of the

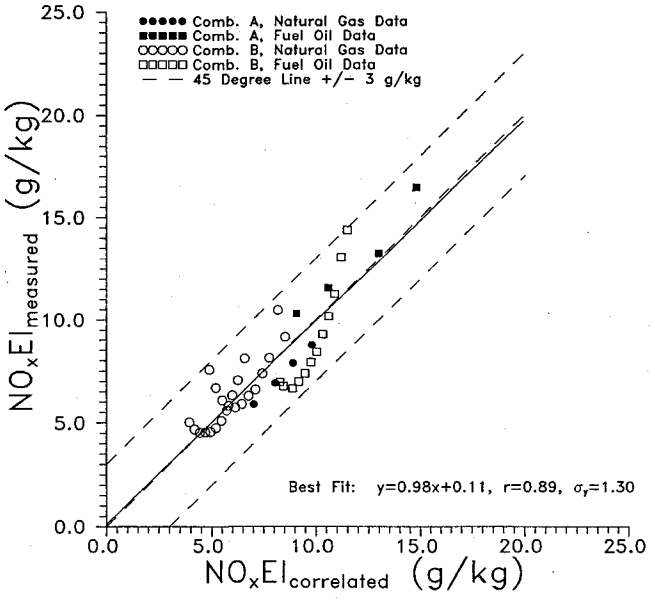

Fig. 2 Characteristic time model least-squares correlation (equation and solid line) of the combustor A and B data without inert injection (symbols). The 45-deg dashed line, with outer dashed lines representing plus and minus one standard deviation, is Eq. (7) with the droplet evaporation time coefficient k_{no} of 0.05, selected to optimize the correlation for the combined combustor A and B data.

new data considered here are within the standard deviation. The correlation quality is good, as the best-fit slope is 0.98 with a y intercept of +0.11, a standard deviation of 1.30 g/kg, and a correlation coefficient of 0.89.

For combustor A, both the natural gas and fuel oil data are correlated linearly about the 45-deg line. However, they are offset as the k_{no} of 0.05 is too large for this combustor. The fuel oil data move above the 45-deg line from well below the 45-deg line as k_{no} is increased from zero.

For combustor B there is a pronounced minimum in both the gas- and oil-fired data. The NO_xEI increase at low load (i.e., near the origin) is not observed for combustor A or for other combustors examined previously.[10] Note that any model modification must relocate data currently on the left of the minimum NO_xEI point to the right of the minimum. The observed trend for this combustor indicates the effective $\tau_{sl,no}$ in Eq. (7) increases for the data at low loads, either through an increase in l_{no} or a decrease in the stoichiometric velocity $V_{\phi=1}$ [Eq. (2)]. An increase in l_{no} clearly requires from Eq. (3) that the effective quench location move downstream past the secondary hole location at low loads, which is unlikely. For the stoichiometric velocity defined in Eq. (5), the fractional flow of air to the primary zone is determined by combustor geometry. Thus, the increase of NO_xEI with decreasing load for combustor B most likely results from use of the stoichiometric flame temperature $T_{\phi=1}$ [see Eq. (5)] at the lowest fuel flows. Decreasing the temperature from $T_{\phi=1}$ at low loads in $\tau_{sl,no}$ can be interpreted as increasing the density and residence time of NO-forming eddies before quenching the NO formation reactions at the secondary hole location. However, the temperature on which τ_{no} is based is not altered, because thermal NO formation rates still are maximum at stoichiometric.

Figure 3 shows the calculated adiabatic equilibrium flame temperatures at the first row of air injection holes for combustor B, normalized with the stoichiometric temperature at full load vs power for one of the sets of natural gas data in Fig. 2. All air and fuel are taken as fully mixed at this station to estimate a local equivalence ratio ϕ. Similar axial normalized temperature profiles are obtained for the other set of natural gas data and for the fuel oil data.

The fully mixed equivalence ratio at the first row of holes is lean at low power and rich at high power, with the stoichiometric condition and peak temperature at approximately the same power as the minimum NO_x value in Fig. 2. For the rich case, it is expected that the fuel will still burn in a diffusion flame near the stoichiometric temperature. In the lean case, using $T_{\phi,1st\ row}$ in place of $T_{\phi=1}$ in the NO_x velocity for the lowest six power points of each of the sets of natural gas data, yields Fig. 4. The low-power data are shifted in line with the high-power data in each case, but as in Fig. 2, the high-power data (higher values of NO_xEI) exhibit a slope higher than the prediction equation. This demonstrates inadequate quenching of thermal NO formation at the secondary holes of combustor B at high powers, as increasing l_{no} in Eq. (2) by 23% will shift the highest point in Fig. 4 to the predicted line.

The two limiting temperature thermal cases ($T_{\phi=1,all}$ and $T_{\phi=1,unif}$) for inert injection, discussed earlier, successfully

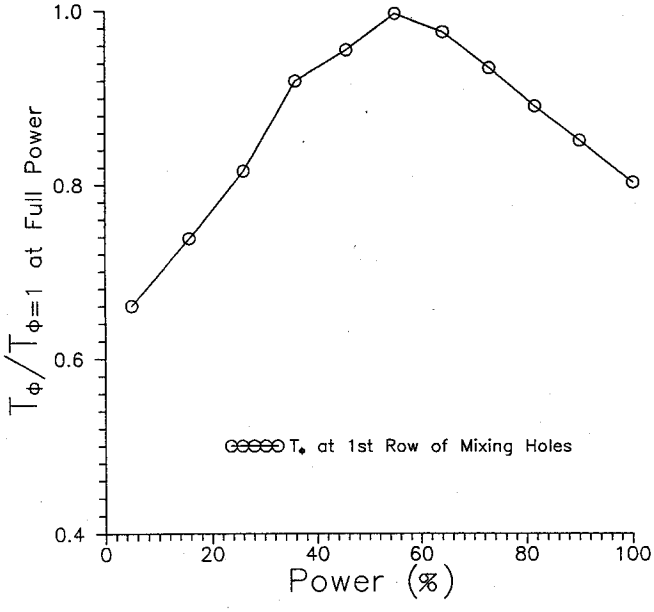

Fig. 3 Computed adiabatic equilibrium temperature for combustor B fired on natural gas at the first row of air addition holes, assuming uniform mixture at the local equivalence ratio, normalized by the stoichiometric value at full load, vs power.

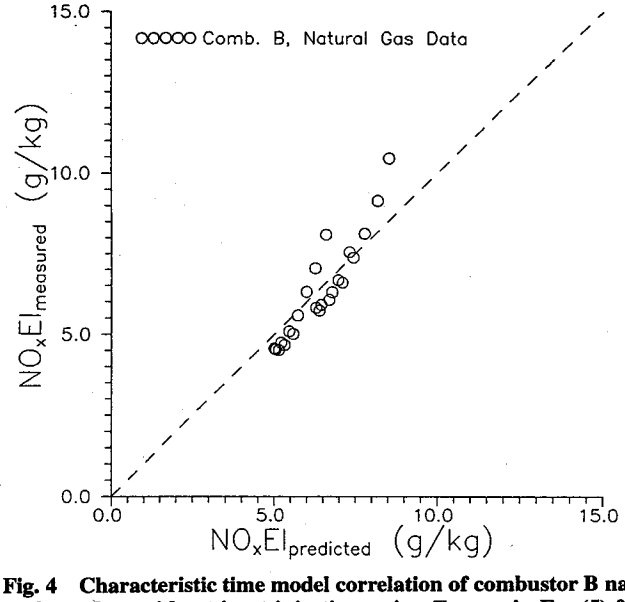

Fig. 4 Characteristic time model correlation of combustor B natural gas data without inert injection, using $T_{\phi,1st\ row}$ in Eq. (5) for the lowest six data in each set. Dashed line is prediction using Eq. (7) with k_{no} = 0.05.

bracketed the measured NO_x reductions in graphs similar to Fig. 1. However, for both combustors the ratio of the measured data to the predictions using $T_{\phi=1,unif}$ varied with power level, while the ratio of the measured values and $T_{\phi=1,all}$ predictions did not. The effective stoichiometric temperature with inert injection that correlated all data was accordingly found to be

$$T_{\phi=1,H_2O} = 0.7T_{\phi=1,all} + 0.3T_{\phi=1} \quad (12)$$

where, in the limit as $\dot{m}_{H_2O}/\dot{m}_{fuel}$ goes to zero, $T_{\phi=1,all} = T_{\phi=1} = T_{\phi=1,H_2O}$. The CTM correlation of all 164 combustor A and B data using $T_{\phi=1,H_2O}$ instead of $T_{\phi=1}$ for both water and steam injection with natural gas and fuel oil is shown in Fig. 5. Evaporation effects were included retaining $k_{no} = 0.05$ in Eq. (7) and assuming the fuel droplet evaporation times were the same as those without inert injection at the appropriate fuel flow rate.

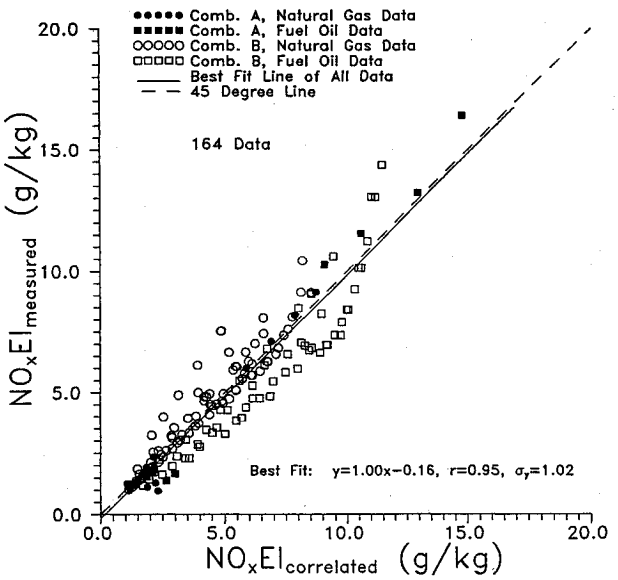

Fig. 5 Characteristic time model performance comparison graph of dry, water-, and steam-injected combustor A and B NO_x data using $T_{\phi=1,H_2O}$. Dashed line is prediction Eq. (7) with $k_{no} = 0.05$; solid line is least-squares correlation of data indicated by symbols.

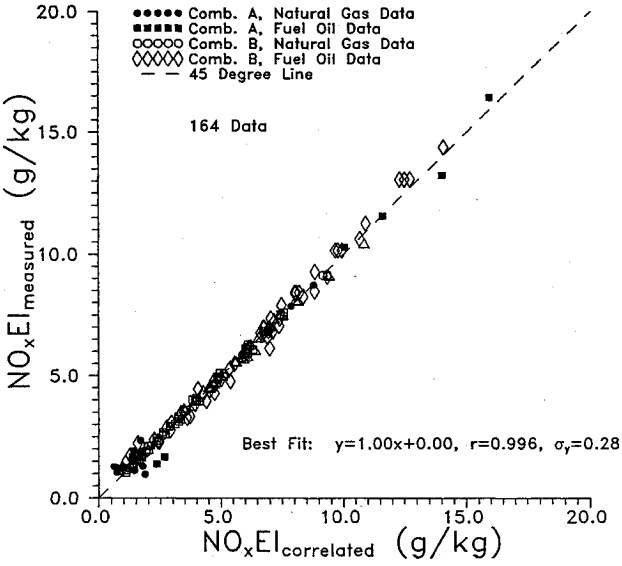

Fig. 6 Measured vs correlated CTM graph of dry, water-, and steam-injected combustor A and B NO_x data with the curvature of the data for combustor B removed empirically and using combustor-specific values of k_{no} in Eq. (7).

The best-fit line shown in Fig. 5 is very close to the correlation originally obtained for dry firing, and the correlation has a standard deviation σ_y of 1.02 g/kg, lower than that for the dry data alone (see Fig. 2). The y intercept (−0.16) is significantly smaller than the standard deviation, and so it may be assumed negligible. The curvature in the combustor B data for each inert-to-fuel flow ratio is responsible for the large standard deviation.

As an example of model fine-tuning for a specific combustor, in Fig. 6 this curvature has been removed empirically by fitting slope [4.5 in Eq. (7)] and y intercept [zero in Eq. (7)] for combustor B at each power setting over the range of inert-to-fuel ratios. In addition, optimal values of k_{no} for each combustor (not reported here) have been incorporated in Fig. 6. With these empirical adjustments, the standard deviation is reduced to 0.28 g/kg [1 g/kg ≅ 11 parts per million volume dry (ppmvd) at 15% O_2].

Conclusions

The characteristic time model for thermal NO_x emissions was modified to account for finite rate evaporation found significant for 100- to 150-MW combustion turbines burning fuel oil. As spray droplet lifetimes increase, NO_x emissions decrease from those computed assuming complete evaporation, because less fuel vapor is available in the region of the combustor where thermal NO forms. One combustor studied here, in contrast to all of those examined previously, exhibited minimum NO_x emissions index at an intermediate load. The CTM was used to show that the increased NO_xEI at lower power for this combustor results from increased residence times, that is, the lower fuel flows and correspondingly smaller heat release rates at light loads result in decreased characteristic flow velocities in the region of NO formation. At high power, NO_xEI values larger than the model prediction for this combustor are because of insufficient airflow through the secondary holes to quench the NO formation reactions in the dilution zone.

Inert injection reduces conventional combustor NO_x emissions primarily by lowering the peak flame temperature. Thus, to correlate these reductions, a modification was required to the stoichiometric flame temperature used to estimate the thermal NO formation rate in the characteristic time model. Two limiting temperatures were hypothesized based on maximum and minimum amounts of water supplied to the stoichiometric eddies in the combustor. The measured inert injection data for both combustors were bounded by the thermal NO_x CTM predictions using these two temperatures.

The effective stoichiometric temperature $T_{\phi=1,H_2O}$ selected to correlate the inert injection data from both combustors represents an injection efficiency of 70% [Eq. (12)]. Figure 6 shows the quality of the results that can be obtained (approximately ±3.2 ppmvd at 15% O_2) if model constants are fine-tuned and the curvature is removed empirically for the combustor exhibiting minimum NO_x emissions at intermediate load. A similar technique could be used as a machine health diagnostic, in lieu of continuous monitors, or to predict emissions once a system has been installed.

Since the same empirical effective stoichiometric temperature correlated the measured NO_x reductions with inert injection for two combustor geometries, two inerts, two fuels, and a wide range of power levels, the assumption that NO is reduced primarily through the thermal effect[21,28] is supported. The leveling off of NO reductions at high inert-to-fuel ratios because of NO produced from nonthermal mechanisms, as suggested by Toof,[22] was not observed in this study. However, measured data were not available for water-to-fuel mass ratios much larger than unity.

The original thermal NO_x CTM prediction equation [Eq. (7) with $k_{no} = 0$] has been extended to include combustors with significant fuel oil evaporation times. Thus, the four-combustor correlation developed by Washam[10,11] is a special case (negligible heterogeneous effects) of Eq. (7), now validated with

data from seven combustors (automotive, aircraft, helicopter, industrial, and utility power generation). Based on results presented here, for predictions, a value of $k_{no} = 0.05$ is recommended. In addition, a method to predict the effectiveness of water or steam injection in reducing NO_x emissions from conventional heavy-duty combustors has been developed, but should be validated with data for other configurations. The 70% injection effectiveness represented by Eq. (12) is obtained from measurements on optimized, fielded machines (i.e., nonoptimal inert injection locations will yield lower values of effectiveness).

Acknowledgments

The authors appreciate funding from ENEL s.p.a. (the major Italian Power Utility), Pisa, Italy; and from CISE s.p.a. (Center for Information, Studies and Experiments), Milan, Italy, under Technical Specification DSM-ST-92-004/Purchase Order 86073. We are grateful to Max De Carli and Vito Marcolongo for their support of the program.

References

[1]Hung, W. S. Y., "A Predictive NO_x Monitoring System for Gas Turbines," American Society of Mechanical Engineers Paper 91-GT-306, June 1991.

[2]Derr, W. S., and Mellor, A. M., "Recent Developments," *Design of Modern Turbine Combustors*, Academic, London, 1990, pp. 477–544.

[3]Mellor, A. M., "Gas Turbine Engine Pollution," *Progress in Energy and Combustion Science*, Vol. 1, Nos. 2/3, 1976, pp. 111–133.

[4]Newburry, D. M., and Mellor, A. M., "Semi-Empirical Predictions and Correlations of NO_x Emissions from Utility Combustion Turbines," American Society of Mechanical Engineers Paper 95-GT-70, June 1995.

[5]Lefebvre, A. H., "Fuel Effects on Gas Turbine Combustion—Liner Temperature, Pattern Factor and Pollutant Emissions," *Journal of Aircraft*, Vol. 21, No. 10, 1984, pp. 887–898.

[6]Rizk, N. K., and Mongia, H. C., "Semianalytical Correlations for NO_x, CO, and UHC Emissions," American Society of Mechanical Engineers Paper 92-GT-130, June 1992.

[7]Tuttle, J. H., Colket, M. B., Bilger, R. W., and Mellor, A. M., "Characteristic Times for Combustion and Pollutant Formation in Spray Combustion," *16th Symposium (International) on Combustion*, The Combustion Inst., Pittsburgh, PA, 1977, pp. 209–219.

[8]Mellor, A. M., "Characteristic Time Emissions Correlations and Sample Optimization: GT-309 Gas Turbine Combustor," *Journal of Energy*, Vol. 1, July–Aug. 1977, pp. 244–249.

[9]Mellor, A. M., "Characteristic Time Emissions Correlations: The T-63 Helicopter Gas Turbine Combustor," *Journal of Energy*, Vol. 1, July–Aug. 1977, pp. 257–262.

[10]Washam, R. M., "Characteristic Time Studies for Conventional Gas Turbine Combustors," M.S. Thesis, School of Mechanical Engineering, Purdue Univ., West Lafayette, IN, 1979.

[11]Mellor, A. M., and Washam, R. M., "Characteristic Time Correlations of Pollutant Emissions from an Annular Gas Turbine Combustor," *Journal of Energy*, Vol. 3, July–Aug. 1979, pp. 250–253.

[12]Tuttle, J. H., Altenkirch, R. A., and Mellor, A. M., "Emissions from and Within an Allison J-33 Combustor. II. The Effect of Inlet Air Temperature," *Combustion Science and Technology*, Vol. 7, No. 3, 1973, pp. 125–134.

[13]Tuttle, J. H., Colket, M. B., and Mellor, A. M., "Characteristic Time Correlation of Emissions from Conventional Aircraft Type Flames," Purdue Univ., Rept. PURDU-CL-76-05, West Lafayette, IN, 1976.

[14]Sawyer, R. F., Cernansky, N. P., and Oppenheim, A. K., "Factors Controlling Pollutant Emissions from Gas Turbine Engines," *Atmospheric Pollution by Aircraft Engines*, CP-125, AGARD, 1973.

[15]Zeldovich, Y. B., "The Oxidation of Nitrogen in Combustion and Explosions," *Acta Physicochimica*, Vol. 21, Sept. 1946, pp. 577–628.

[16]Godsave, G. A. E., "Studies on the Combustion of Drops in a Fuel Spray—The Burning of Single Drops of Fuel," *4th Symposium (International) on Combustion*, Williams and Wilkins Co., Baltimore, MD, 1953, pp. 818–830.

[17]Frössling, N., "On the Evaporation of Falling Droplets," *Gerlands Beitrage zur Geophysik*, Vol. 52, Feb. 1938, pp. 170–216.

[18]Leonard, P. A., and Mellor, A. M., "Correlation of Gas Turbine Combustor Efficiency," *Journal of Energy*, Vol. 7, Nov.–Dec. 1983, pp. 556–602.

[19]Fenimore, C. P., *13th Symposium (International) on Combustion*, The Combustion Inst., Pittsburgh, PA, 1971, pp. 373–380.

[20]Malte, P. C., and Pratt, D. T., "The Role of Energy-Releasing Kinetics in NO_x Formation: Fuel Lean, Jet Stirred CO–Air Combustion," *Combustion Science and Technology*, Vol. 9, Nos. 5 and 6, 1974, pp. 221–231.

[21]Touchton, G. L., "Influence of Gas Turbine Combustor Design and Operating Parameters on Effectiveness of NO_x Suppression by Injected Steam or Water," *Journal of Engineering for Gas Turbines and Power*, Vol. 107, Oct. 1985, pp. 706–713.

[22]Toof, J. L., "A Model for the Prediction of Thermal, Prompt, and Fuel NO_x Emissions from Combustion Turbines," *Journal of Engineering for Gas Turbines and Power*, Vol. 108, April 1986, pp. 340–347.

[23]Bahr, D. W., and Lyon, T. F., "NO_x Abatement via Water Injection in Aircraft-Derivative Turbine Engines," American Society of Mechanical Engineers Paper 84-GT-103, June 1984.

[24]Gleason, C. C., and Rogers, D. W., "Ambient Humidity Correction Factor for Gas Turbine Oxides of Nitrogen Emissions," General Electric TM 73-803, 1973.

[25]Hung, W. S. Y., "Accurate Method of Predicting the Effect of Humidity or Injected Water on NO_x Emissions from Industrial Gas Turbines," American Society of Mechanical Engineers Paper 74-WA/GT-6, Nov. 1974.

[26]Shaw, H., "The Effect of Water on Nitric Oxide Production in Gas Turbine Combustors," American Society of Mechanical Engineers Paper 75-GT-70, June 1975.

[27]Washam, R. M., and Mellor, A. M., "Correlation Technique for Ambient Effects on Oxides of Nitrogen," *Journal of Aircraft*, Vol. 16, No. 9, 1979, pp. 626–631.

[28]Touchton, G. L., "An Experimentally Verified NO_x Prediction Algorithm Incorporating the Effects of Steam Injection," *Journal of Engineering for Gas Turbines and Power*, Vol. 106, Nov. 1984, pp. 833–839.

[29]Reynolds, W. C., "STANJAN Version 3.93," Dept. of Mechanical Engineering, Stanford Univ., Stanford, CA, 1987.

[30]Newburry, D. M., and Mellor, A. M., "Characteristic Time Model Correlation of NO_x Emissions from Lean Premixed Combustors," American Society of Mechanical Engineers Paper 95-GT-135, June 1995.

[31]Derr, W. S., and Mellor, A. M., "Characteristic Times for Lean Blowoff in Turbine Combustors," *Journal of Propulsion and Power*, Vol. 3, No. 4, 1987, pp. 377–380.

[32]Hilt, M. B., and Waslo, J., "Evolution of NO_x Abatement Techniques Through Combustor Design for Heavy-Duty Gas Turbines," *Journal of Engineering for Gas Turbines and Power*, Vol. 106, Nov. 1984, pp. 825–832.

[33]Elkotb, M. M., El-Sayed Mahdy, M. A., and Montaser, M. E., "Investigation of Externally Mixing Air Blast Atomizers," *Proceedings of the 2nd International Conference on Liquid Atomization and Sprays*, Univ. of Wisconsin, Madison, WI, 1982, pp. 107–115.

[34]Lefebvre, A. H., *Atomization and Sprays*, Hemisphere, New York, 1989.